ASEAN Engineering Journal

Full Paper

A DUAL-HYDRAULIC SYSTEM FOR HIGH HYDROSTATIC PRESSURE GENERATION IN INDETERMINATE WATER VOLUMES

Huu Nhan Nguyen[a,b], Hai Dang Ho[a,b], Cong Toai Truong[a,b], Van Tu Duong[a,b], Tan Tien Nguyen[a,b], Huy Hung Nguyen[c*]

[a]Key Laboratory of Digital Control and System Engineering (DCSELab), Faculty of Mechanical Engineering, Ho Chi Minh City University of Technology (HCMUT), 268 Ly Thuong Kiet Street, Dien Hong Ward, Ho Chi Minh City, Vietnam.
[b]Vietnam National University Ho Chi Minh City, Linh Xuan Ward, Ho Chi Minh City, Vietnam
[c]Faculty of Engineering and Technology, Saigon University, Ho Chi Minh City, Vietnam

Article history
Received
12 August 2025
Received in revised form
17 October 2025
Accepted
15 January 2026
Published online
31 August 2026

*Corresponding author
nhhung@sgu.edu.vn

Graphical abstract

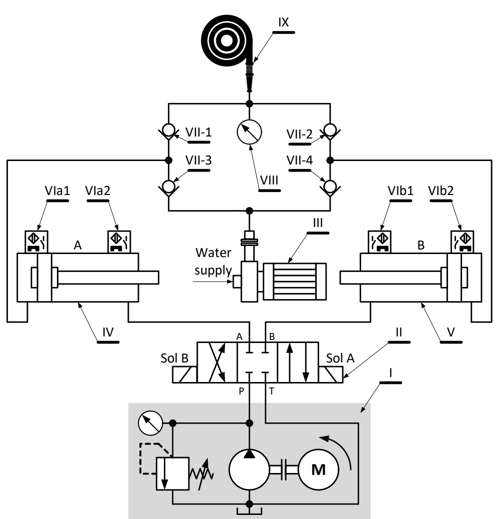

Abstract

Hydrostatic pressure testing is a significant procedure for evaluating fire protection equipment's structural integrity and leak resistance, particularly devices with flexible structures and variable internal volumes such as fire hoses. Instability, safety concerns, and environmental risks hinder conventional pressure generation methods relying on compressed air or hydraulic oil. This study is devoted to introducing a novel dual hydraulic actuation system (D-HAST) that employs water as the working fluid. By substituting compressed air and hydraulic oil, the D-HAST effectively mitigates pressure fluctuations arising from air compressibility and eliminates leakage risks associated with hydraulic oil, thereby establishing a safer and more environmentally sustainable framework for hydrostatic pressure testing. The system leverages two double acting cylinders operating in an alternating compression mode under a finite state machine (FSM) control scheme. The system architecture, component sizing methodology and control logic are systematically developed to achieve rapid pressurization, stable pressure maintenance and real time leakage compensation. A laboratory-scale prototype, designed to ISO 4642:2015 standards, was experimentally validated under both low- and high-leakage conditions. Results show that under low-leakage scenarios, the D-HAST achieved the target pressure within 120 s and maintained stability (±0.02 MPa) for 180 s, while high-leakage tests revealed extended pressurization times (964÷2675 s) and clear differentiation between compliant and defective hoses. The findings confirm that the proposed D-HAST offers a safe, precise, and environmentally sustainable solution for hydrostatic pressure testing, with strong potential for industrial deployment and adaptation to various leakage rates and expansion capacities.

Keywords: hydrostatic pressure testing; fire protection equipment; dual-hydraulic actuation; finite state machine control; leakage compensation

1.0 INTRODUCTION

Fire protection equipment (FPE) [1] testing is a critical factor in ensuring the safety of people and property before these products are released into the market [2]. Conduct thorough testing to identify potential defects and ensure equipment operational reliability in emergency situations [3]. This testing process is not only to comply with international safety standards but also to help reduce the risk of fire, protecting life and property. FPE testing is a mandatory requirement for organizations and manufacturing companies to ensure that products meet safety standards and comply with legal regulations before being put into use [4]. Several studies on fire protection equipment (FPE) quality [5, 6] assurance have highlighted a notable increasing trend in the demand for the quality of these devices.

With automation, FPE inspections gain in efficiency, sharpen accuracy, and narrow opportunities for error. Crucially, automated rigs run standardized procedures in line with international norms, producing results that are both fast and repeatable; the net effect is lower time and resource use than under manual testing [3]. At the same time, data capture becomes systematic: records are timestamped, stored, and retrieved with ease, helping organizations demonstrate compliance with legal and safety requirements. The practical payoff is greater equipment reliability and, by extension, safer workplaces and communities [2].

Recent studies have focused on applying automation in the FPE testing process. Studies [7] and [8] introduce the design of a mobile robot capable of automatically assessing the quality, or more precisely, the power of fire extinguishers, based on the standards ISO 7165: 2009 [9] and ISO 11601: 2017 [10]. Additionally, study [11] develops a control system and algorithm to measure and evaluate the K-factor of fire sprinklers, a critical component in FPE systems, according to ISO 6182: 2014 [12]. Study [13] proposes a method for testing the burst pressure of powder fire extinguishers, using a cylinder with two compartments for water and oil to increase and maintain pressure, in accordance with ISO 11601: 2017 [10]. Furthermore, study [14] presents a gas furnace identification method to develop a model using experimental data, employing two approaches: the bilinear model and the first-order model with dead time. These studies reflect an increasing trend toward the application of automation in FPE testing, opening up significant prospects for improving the efficiency and accuracy of fire protection equipment inspections.

Hydrostatic pressure testing is a standard method to verify structural integrity and leak-tightness in fire-protection equipment. Typical specimens include fire hoses, valves, high-pressure extinguishers, and water pipelines [4]. These devices often run at elevated pressure; in critical incidents, their performance can determine the protection of life and property. Readiness and effectiveness follow from one premise: integrity must hold under load [4, 15]. Beyond these material concerns, conventional hydrostatic testing in fire protection equipment inspection still faces broader limitations. In practice, pressure verification is usually performed under static loading conditions and does not accurately reproduce the transient fluctuations that occur during real firefighting operation. The process relies heavily on manual valve control and offers limited means for automated compensation when leakage appears. As a result, test outcomes can vary among laboratories, making it difficult to ensure consistency and traceability across different setups. These aspects underline the need for a safer and more controlled approach that maintains stability and repeatability while minimizing operator dependency.

International standards such as ISO 6182-1:2014 [12] for sprinkler systems, NFPA 1962 [16] for fire hoses and ISO 4642:2015 [17, 18] for semi-rigid pipes require hydrostatic pressure testing to verify durability and operational performance, and these standards set out both the step-by-step procedures and the minimum pressure levels to be applied so that each device, before it enters service, is subjected to a rigorous and reproducible evaluation. By prescribing test pressures that typically range between 1.5 and 2.5 times the rated working pressure, with the exact multiplier determined by the device category and its intended use, these documents establish the framework that sustains the safety and effectiveness of fire protection systems [4, 19]. While these standards provide a solid framework for ensuring product reliability, their scope and emphasis differ in notable ways. The standards ISO 6182 and ISO 4642 focus on laboratory based qualification, prescribing controlled pressurization rates and precise hold times to secure repeatable results under ideal conditions. In contrast, NFPA 1962 is oriented toward periodic field inspection and maintenance, allowing procedural flexibility that better reflects practical service environments. This divergence in testing philosophy illustrates that fire protection equipment must be evaluated under both stable laboratory settings and variable field conditions, highlighting the importance of adaptable testing systems capable of maintaining accuracy across different scenarios.

Although hydrostatic pressure testing is widely accepted, the conventional means of generating pressure in test rigs, which typically rely on compressed air or on hydraulic oil as the working fluid, still exhibit inherent limitations that undermine stability, accuracy, and environmental safety. Although these methods have been employed for many years, each exhibits inherent limitations that compromise accuracy, safety, and environmental sustainability during testing [15].

Compressed air, though widely used and easy to deploy, introduces air compression effects, leading to unstable pressure during testing. The compressibility of air drives pressure oscillations that erode accuracy and reduce the sensitivity of leak detection, rendering the assessment of actual durability uncertain. Reaching the desired pressure level also tends to take longer. Hydraulic oil solves neither the risk nor the cleanup problem: a leak can discharge hazardous fluid, cleanup is complex and costly, and the environmental impact can be severe. Moreover, hydraulic oil poses a fire hazard, which is especially concerning when testing fire protection equipment, where cleanliness and safety are of paramount importance [15].

Therefore, a more efficient, sustainable, and environmentally responsible approach to hydrostatic pressure testing is urgently required. To address these challenges, this study proposes a dual hydraulic actuation system (D-HAST), using water as the working fluid. Eliminating compressed air and hydraulic oil addresses the root cause of pressure oscillations and reduces safety and environmental exposure. The D-HAST is arranged as two hydraulic cylinders operating in alternation under coordinated control, thereby generating a continuous and stable pressure signal for water-filled specimens whose internal volume may change or be undetermined. The design is engineered to deliver fast pressurization, stable pressure regulation, and greater sensitivity to small leaks, thereby addressing the principal shortcomings of conventional testing systems.

Because water is effectively incompressible at the pressures of interest, the test rig can maintain a smooth, stable pressure profile rather than the fluctuations observed with air, resulting in more reliable measurements. This choice of working fluid also offers practical benefits—safe handling, wide availability, and a low environmental footprint—making it suitable for industrial testing while supporting sustainability objectives in the fire protection sector. The proposed system is engineered to accommodate a variety of testing scenarios, including flexible fire hoses with variable internal volumes. To achieve this, it integrates advanced control mechanisms, most notably a finite state machine (FSM)-based controller, enabling discrete control and coordinated operation of multiple devices [20], [21]. This ensures stable pressure maintenance and timely compensation for any leakage during testing.

The methodology for selecting and sizing the D-HAST's key components— including hydraulic cylinders, control valves and sensors is presented in detail. Component selection is guided by the target pressure, the desired pressurization rate and the characteristics of the specimen. With these inputs optimized, the proposed system produces the required pressure profile and adapts to variations in leakage rate, yielding a comprehensive platform for evaluating fire-fighting devices.

To substantiate the proposed approach, this research constructed a laboratory-scale prototype conforming to ISO 4642:2015 and evaluated it experimentally. Across hoses of different types and leakage magnitudes, the proposed system maintained the target pressure by compensating for losses and, in the process, clearly distinguished units that met requirements from those that did not. The evidence supports D-HAST as a safe, accurate, and environmentally responsible option for hydrostatic testing. The main contributions of this study are as follows:

- Introduction of a novel principle for hydrostatic pressure generation using two double— acting cylinders with water as the working medium, capable of compensating for leakage in devices with varying leakage rates and fill volumes.
- Development of a generalized methodology for selecting and constraining the parameters of components in the D-HAST.
- Applying FSM-based control to manage device states and enable coordinated system state transitions.

2.0 METHODOLOGY

2.1 D-HAST Architecture

To address the challenge of generating and maintaining high hydrostatic pressure in enclosed water-filled specimens with indeterminate expansion capacity, particularly under conditions involving leakage and nonlinear deformation, as in fire hoses, this study proposes a dual hydraulic actuation system (D-HAST). The proposed system employs two reciprocating hydraulic cylinders operating in an alternating compression mode, enabling continuous and stable pressurization with real-time leakage compensation. This configuration effectively meets the technical requirements of fire protection specimen testing.

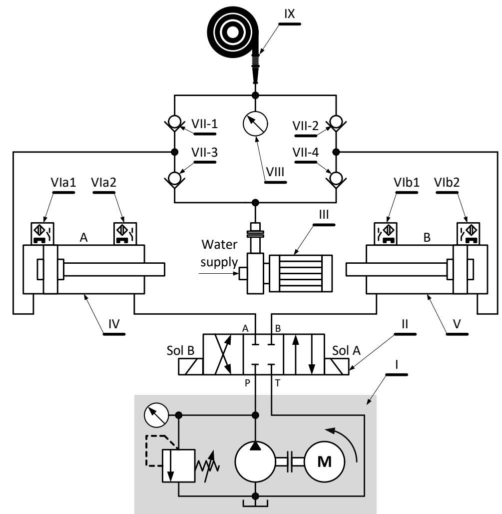

Figure 1 Specimen and piping diagram illustrating the D-HAST

Figure 1 shows the schematic diagram of the proposed D-HAST, comprising nine components: a hydraulic power unit (I), a directional control valve (II), a water pump motor (III), two double-acting hydraulic cylinders (IV) and (V), four position sensors (VIa1), (VIa2), (VIb1), (VIb2), four check valves (VII-1), (VII-2), (VII-3), (VII-4), a pressure sensor (VIII), and a fire hose reel (IX) representing the specimen to be tested.

The inlet of the hydraulic power unit (I) is connected to port P of the directional control valve (II) via a fluid conduit, supplying hydraulic oil through either port A or B depending on the state of solenoid coil A or solenoid coil B. Ports A and B of the directional valve are connected respectively to the rod-end chambers of hydraulic cylinders (IV) and (V). The inlet of valve (VII-1) is connected to the outlet of valve (VII-3) and routed to the cap-end chamber of hydraulic cylinder A. Similarly, the inlet of valve (VII-2) is connected to the outlet of valve (VII-4) and routed to the cap-end chamber of hydraulic cylinder B. The inlets of valves (VII-3) and (VII-4) are interconnected and connected to the water pump motor (III), while the outlets of valves (VII-1) and (VII-2) are simultaneously connected to the fire hose reel. The pressure gauge (sensor) (VIII) is installed to monitor the hydrostatic pressure of the fire hose reel. The position sensors (VIa1), (VIa2), (VIb1), and (VIb2) are mounted in appropriate locations to detect the retraction and extension strokes of hydraulic cylinders A and B.

2.2 Generalized Design Formulas for Specimen Selection Based on Target Pressure and Pressurization Rate

The proposed system is designed for applications requiring the generation and maintenance of high hydrostatic pressure within a sealed, water-filled chamber with an undefined expansion volume. Simultaneously, the pressure increase rate also meets the requirements of various test scenarios. Therefore, based on two fundamental input parameters— the maximum test pressure P(MPa) and the maximum pressure increase rate v(MPa/s)— this study introduces a method for selecting appropriate specimens for machines implementing this pressure-boosting system.

The hydraulic power unit (I) serves as the primary energy source for the proposed system, and the hydraulic oil flow rate

$Q_d(cm^3/s)$ is calculated based on the kinematic requirements of the piston as follows [22]:

$$Q_d = A_r v_p(t), \quad (1)$$

where, $A_r = \frac{\pi}{4}\left(D_c^2 - d_r^2\right)(cm^2)$ is the cross-sectional area of the hydraulic cylinder; D_c is the outer diameter of the piston; d_r is the diameter of the piston rod; $v_p(t)(cm/s)$ is the piston velocity, which depends on the required pressure increase rate [22, 23]:

$$v_p(t) = \frac{V(t)}{K_w A_c} v, \quad (2)$$

where $V(t)(cm^3)$ is the volume of the cap-end chamber of the hydraulic cylinder at time t; $A_c(cm^3)$ is the cross-sectional area of the piston on the cap-end side; $K_w(MPa)$ is the volumetric compression ratio of water.

Thus, the selected hydraulic power unit provides a minimum flow rate of Q_d, and its output pressure reaches at least the following value [22]:

$$P_r(t) = \frac{\frac{m_p dv_p(t)}{dt} + b_p . v_p(t) + A_c P}{A_r}, \quad (3)$$

where, $m_p(kg)$ is the mass of the piston assembly; $b_p(kg/s)$ is the viscous damping coefficient of the piston.

The hydraulic directional control valve (II) is a four-way directional valve with ports A, B, P, and T, featuring either two or three working positions. It is actuated by two solenoids using electrical signals. The flow capacity of the valve is determined by [24]:

$$Q_{val} = C_d A_{or} \sqrt{\frac{2(P_s - P_r)}{\rho_d}}, \quad (4)$$

where, C_d is the flow coefficient of the valve; $A_{or}(cm^2)$ is the effective open cross-sectional area of the valve port; $P_s(MPa)$ is the supply pressure; $\rho_d(kg/cm^3)$ is the hydraulic-oil's density.

To meet the D-HAST requirements, the hydraulic directional control valves have a sufficiently large effective cross-sectional area to ensure a minimum flow rate of $Q_{val} \geq Q_d$. This component operates with continuous state switching during the operation of the proposed system; therefore, it requires high durability and fast response time.

The water pump (III) is responsible for filling the test specimen with water. Its flow rate determines the water filling speed, while the pressure generated by the pump not only shortens the time required to increase hydrostatic pressure inside the test specimen but also facilitates the full extension of the hydraulic cylinder piston. Since the required water volume varies depending on the specific test specimen, the pump's flow rate is selected to suit the testing purpose. However, it is required to meet a minimum flow rate of Q_w to ensure a timely water supply for the pressurization process and complete piston extension [22, 23]:

$$Q_w = A_c v_p(t). \quad (5)$$

The hydraulic cylinders (IV) and (V) are responsible for compressing the sealed water-filled chamber, thereby increasing the hydrostatic pressure applied to the test specimen. The volume of the hydraulic cylinders determines the operating duration of each phase [22].

$$V(t) = A_c\left(L_c - x(t)\right), \quad (6)$$

where, $A_c = \frac{\pi}{4} D_c^2 (cm^2)$ is the piston area on the cap-end side; $L_c(cm)$ is the length of the hydraulic cylinder; $x(t)(cm)$ is the instantaneous stroke of the piston.
To achieve the target pressure, the liquid compression law is applied as follows [22]:

$$P = P_{w0} + \frac{K_w}{V(t)} \Delta V(t), \quad (7)$$

where, $P_{w0}(MPa)$ is the initial pressure of the water in the compression chamber; $\Delta V(t)(cm^3)$ is the volume change of the water due to compression at time t.

Therefore, the selection of the hydraulic cylinder ensures a suitable compression volume to achieve the target pressure P without exceeding the piston stroke limit. An excessively long cylinder reduces the pressure increase rate due to the following reasons [22]:

$$v = \frac{K_w A_c}{V(t)} v_p(t). \quad (8)$$

Conversely, an overly short cylinder may not provide sufficient compression volume. Therefore, it is essential to carefully optimize the trade-off between stroke length, cylinder diameter, and pressure increase capability.

Position sensors (VIa1), (VIa2), (VIb1), (VIb2): These sensors are used to detect the retracted and extended positions of the hydraulic cylinders. Possible implementations include Hall-effect sensors mounted on the cylinder body to detect an internal magnetic component, or eddy current sensors used to detect the position of the cylinder rod.

Check valves (VII-1), (VII-2), (VII-3), and (VII-4) allow water to flow in only one direction. The series-connected check valve branches ensure that water from the pump (III) can be supplied to the hydraulic cylinder and the test specimen, while simultaneously preventing reverse flow of hydrostatic pressure, which could otherwise damage the pump. To meet these requirements, the check valve can withstand a minimum pressure equal to the target hydrostatic pressure P applied to the test specimen. Additionally, the nominal flow capacity of the valves exceeds Q_w, both the materials and structural design of the valves ensure high sealing performance and long-term durability.

Pressure Gauge (Sensor) (VIII): This component measures the hydrostatic pressure inside the fire hose reel. To enable automatic pressure control, the sensor should be of the type that provides electrical signal feedback and interfaces with a programmable control device, such as a PLC, for signal processing and regulation.

The fire hose reel (IX) represents the firefighting specimens or devices required for quality inspection and testing. This specimen varies in terms of diameter, length, working pressure, and burst pressure.

2.3 Hydrostatic Pressure Control Strategy

In the D-HAST, maintaining stable pressure, compensating for leakage, and controlling the operation cycle in real-time are important requirements that need to be fulfilled. To achieve these goals, this study proposes a decision-making controller based on a Finite State Machine (FSM), which serves as the central coordinator for the entire system, including two hydraulic cylinders, an oil pump, a water pump, and related components. The FSM controller is structured using a five-component model: FSM=(Σ, S, s_0, δ, O), where, Σ denotes the set of input signals; S represents the set of operational states of the D-HAST; s_0 is the initial state; δ is the state transition function, which defines the rule for determining the next state based on the current state and a specific combination of input conditions and corresponding outputs; and O denotes the set of output signals of the proposed system.

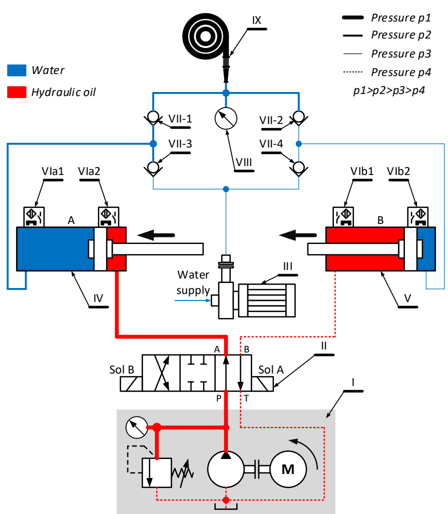

Figure 2 A diagram illustrating the operating state of phase A - stage 2

The pressure generation and maintenance process in the D-HAST is divided into two phases, comprising a total of seven operational states. The first phase includes two states:

- State 0 (Idle): The proposed system is in a standby mode and performs no operation.
- State 1 (Water filling): The water pump is activated to fill the sealed chamber of the test device while simultaneously supplying water to the cap-end chambers of both hydraulic cylinders A and B. This state ends when the pressure inside the D-HAST system reaches the maximum discharge pressure of the water pump.

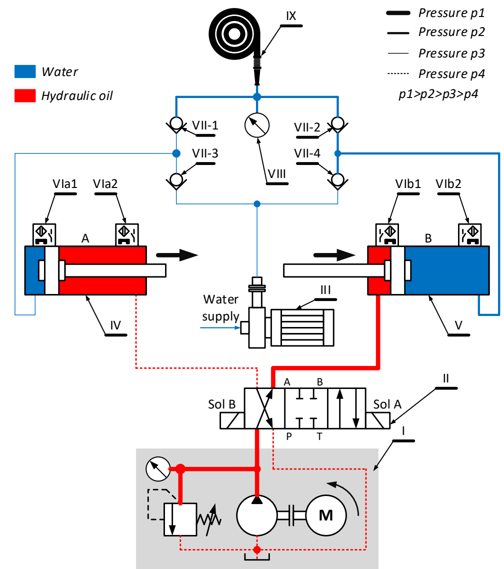

Figure 3 A diagram illustrating the operating state of phase B - stage 2

The second phase is subdivided into two sub-phases: Phase A and Phase B, characterized by alternating solenoid valves A and B switching. This switching controls the compression of hydraulic cylinders A and B, thereby cyclically increasing the hydrostatic pressure in fire hose. The connection diagrams and corresponding hydraulic flow paths for these two sub-phases are illustrated in Figure 2 and Figure 3. The second phase consists of the following states:

- State 2A (Compression cylinder A): Solenoid valve A is activated and the oil pump drives the piston of cylinder A to retract. Water from the rear chamber is forced through a check valve into the test device, generating hydrostatic pressure. Once cylinder A is fully retracted (detected by sensor VIa1), the D-HAST transitions to the refill state for cylinder A.
- State 3A (Refill cylinder A): The water pump is activated to refill the drive chamber of cylinder A. This state ends when the piston reaches its maximum extension (detected by sensor VIa2).
- State 2B (Compression cylinder B): Similar to State 2A but for cylinder B. Solenoid valve B is activated and the oil pump drives piston B to retract, pushing water into the test device. The state ends when sensor VIb1 detects that cylinder B is fully retracted.
- State 3B (Refill cylinder B): The water pump refills the rear chamber of cylinder B through a check valve. When sensor VIb2 detects that piston B has reached its maximum stroke, the D-HAST transitions back to State 2A to begin a new compression cycle.
- State 4 (Pressure holding): When the hydrostatic pressure in the test device reaches the desired threshold, the D-HAST enters the pressure holding state. Compression operations are paused, and the pressure is continuously monitored for potential leakage. If a sudden pressure drop is detected, D-HAST returns to State 2A to perform compensatory compression.

The D-HAST utilizes a set of ten input signals, denoted as $\sigma_i \in \Sigma$, i=0÷9, to enable real-time control and monitoring of the operation process. Specifically, σ_0 is the signal requesting the initiation of the test procedure; σ_1 indicates that the pressure has reached the high discharge threshold of the water pump; σ_2 and σ_3 are signals from sensors VIa1 and VIb2, confirming that cylinders A and B are fully retracted, respectively. Signals σ_4 and σ_5, from sensors VIa2 and VIb1, indicate that the corresponding cylinders have completed their extension strokes. Signal σ_6 confirms that the hydrostatic pressure in fire hose has reached the target level, while σ_7 serves as a warning when a significant pressure drop is detected before reaching the desired threshold. Finally, σ_8 confirms that the pressure holding time has been fulfilled, and σ_9 signals a request to terminate the pressure increase process.

The D-HAST consists of four key actuating devices that play a direct role in the pressure build up and maintenance process. The operational state of each device is encoded using binary values: bit 0 represents the inactive (OFF) state, while bit 1 indicates the active (ON) state. Out of the sixteen possible output combinations, a set of ten feasible outputs has been selected to represent the D-HAST's output space. These selected outputs are detailed in the following Table 1.

Table 1 Set of Outputs with Respect to States

Outputs O_i	Solenoid A	Solenoid B	Water Pump	Oil Pump	Hexadecimal
1	0	0	0	0	0_H
2	0	0	1	0	2_H
3	0	1	0	1	5_H
4	0	1	1	1	7_H
5	1	0	0	1	9_H
6	1	0	1	1	B_H

The state set of the D-HAST system comprises seven discrete states, defined sequentially according to the control process described in the previous sections. The state transition function $\delta: \Sigma \times S \rightarrow S \times O$ governs how D-HAST moves from one state to the next, based on the current input signal combination, and simultaneously generates the corresponding control output O_i.

Table 2 presents the detailed logic rules of the FSM. Each row corresponds to a current state, specifying the input conditions and the resulting next state. A dash indicates that the proposed system remains in the current state if no transition condition is met.

Table 2 State Transition Table

State	σ_0	σ_1	σ_2	σ_3	σ_6	σ_7	σ_8	σ_9	σ_4&σ_3	σ_5&σ_2
0	1	-	-	-	-	-	-	-	-	-
1	-	2A/2B	-	-	-	-	-	-	-	-
2A	-	-	3A	-	4	4	-	-	-	-
2B	-	-	-	3B	4	4	-	-	-	-
3A	-	-	-	-	-	-	-	-	2A	-
3B	1	-	-	-	-	-	-	-	-	2B
4	1	-	-	-	-	-	0	0	-	-

To provide a visual representation of proposed-system's operation, a state diagram in Figure 4 is constructed to illustrate the state transitions under the influence of input signals. In this diagram, each node represents a state and is connected to the next state via a labeled edge indicating the input signal σ_i and the corresponding control action O_i. The initial state of the FSM is defined as State 0 (Idle).

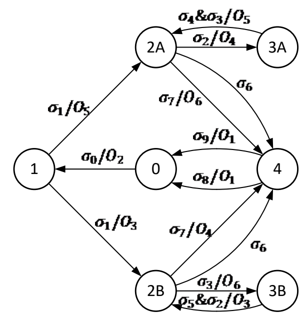

Figure 4 State diagram of FSM

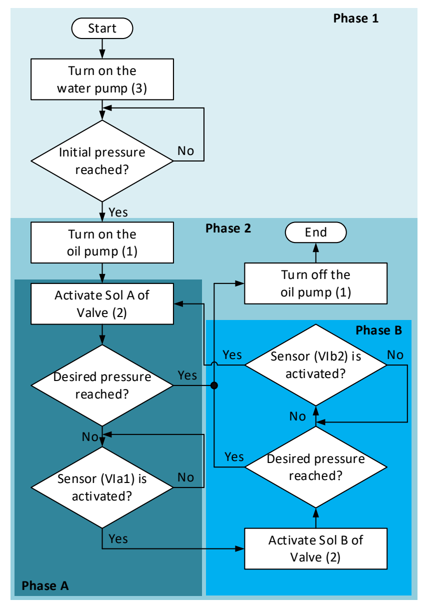

Figure 5 A flowchart illustrating the control algorithm of D-HAST

To support the practical implementation of the control system, Figure 5 provides a flowchart illustrating the operational sequence of proposed system. This flowchart outlines the conditional processing flow from the start of the test, through the water filling process, into the compression phases using cylinders A and B, and ending when the required pressure is reached or the holding time has elapsed.

3.0 RESULTS AND DISCUSSION

Figure 6 presents a system prototype developed based on the proposed principle. The hydraulic power unit (I) is selected as a 380 V three phase electric system with a power output of 2.2 kW, a hydraulic pump displacement of 3.3 cc/rev, an oil reservoir capacity of 8 liters, and a pump motor speed of 1450 revolutions per minute. Additionally, the hydraulic power unit is equipped with components such as a pressure gauge and a relief valve for system monitoring and protection. The water pump (III) provides a flow rate of 2 m^3/min with a corresponding pressure head of 90 meters of water column. The hydraulic cylinders employed have an outer diameter of 100 mm, a piston diameter of 50 mm, and a stroke length of 150 mm.

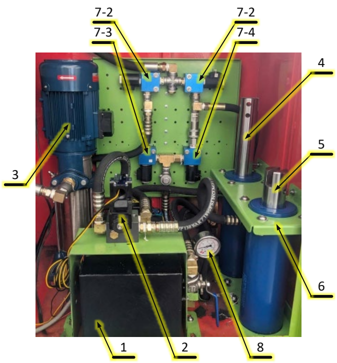

Figure 6 The D-HAST was implemented based on the proposed principle

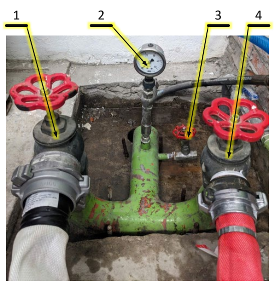

Figure 7 Connector assembly for mounting the fire hose under test
(1) - Connector for the first fire hose, (2) - Pressure gauge, (3) - Pressure relief valve, (4) - Connector for the second fire hose

There is a slight modification compared to the proposed principle, whereby the actual piping and equipment system utilizes four two-way, two-position valves integrated with low-leakage check valves instead of the four independent check valves originally proposed. This modification allows the proposed system to flexibly supply water to either hydraulic cylinder branch as required.

The specimen selected for this test is a fire hose that complies with ISO 4642:2015 for hydrostatic pressure testing. The hose has a nominal working pressure of 1.6 MPa; according to the test requirements, the hydrostatic pressure reaches at least 1.25 times the working pressure, equivalent to 2.0±0.1 MPa. The hose is connected to the piping and equipment system via a dedicated connector assembly, as illustrated in Figure 7. This connector assembly is designed with two outlets, enabling simultaneous testing of two hoses to improve testing productivity and efficiency. Additionally, the connector assembly is equipped with a pressure gauge for monitoring and calibrating the proposed system throughout the test, along with a ball valve for pressure release to ensure safety when required.

The experimental process consists of two separate and independent tests designed to assess both the performance of the prototype and the condition of the specimen under different scenarios. In the first test, hydrostatic pressure is applied to the proposed system without connecting the specimen or vehicle subject to inspection. The objective of this test is to verify the operational status of the prototype itself and to evaluate any potential internal pressure losses before conducting tests on the actual specimen. The second test involves applying and maintaining hydrostatic pressure to the fire hose, and the specimen is to be inspected. In this test, the hose is connected to the proposed system, pressure is increased to the required level, and then maintained for a defined period to observe stability and detect possible leakage. The specimen is classified as having significant leakage if stable pressure cannot be maintained throughout the test duration. The implementation of these two independent tests allows for observing the behavior of the setup when connected to a specimen with unknown internal water volume, as well as assessing the setup's capability to compensate for pressure losses caused by significant leakage in the tested specimen.

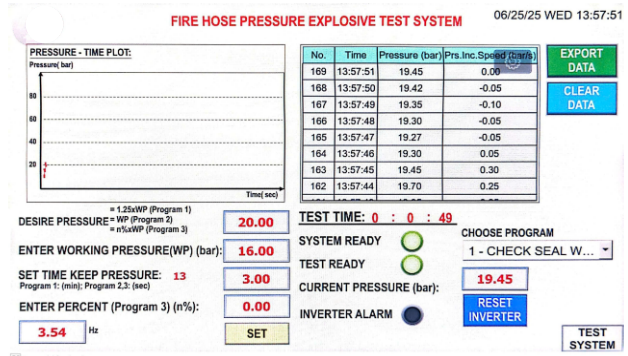

Figure 8 HMI for the testing system

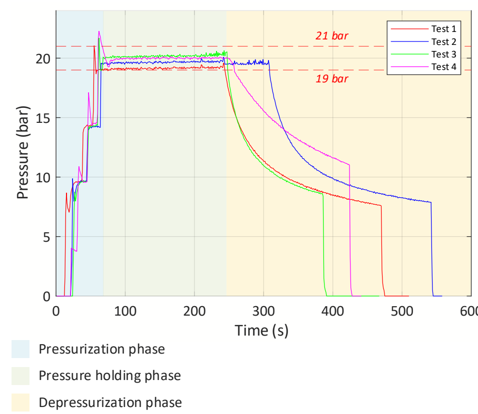

Figure 9 Hydrostatic pressure at the hose under low-leakage conditions

Figure 8 shows the human machine interface (HMI) of the proposed system, which allows operators to set test parameters and observe the pressurization process in real time. The interface presents key indicators such as target and current pressure, cylinder status and control buttons for starting or stopping the test. This design simplifies operation, enables data recording throughout the process, supports consistent and repeatable testing of the D-HAST.

Figure 9 illustrates the variation of hydrostatic pressure in the proposed system under low-leakage conditions, recorded over four independent test iterations. The hydrostatic pressure curves are nearly identical across the trials and can be categorized into three main phases: pressurization, steady pressure holding for 180 seconds, and depressurization to zero.

During the initial phase, the hydrostatic pressure starts at nearly 0 MPa and increases relatively quickly, reaching the target level within approximately 120 seconds. This rapid rise is attributed to the small internal volume of the sealed system and the effective performance of the water pump. However, towards the end of this phase, due to the proposed system's high tightness, even a slight displacement of the hydraulic cylinder can result in a sharp pressure spike, leading to overshoot. This overshoot phenomenon is further intensified by the response delay of the solenoid valves and the inertial effect of the hydraulic fluid, which causes the pressure to continue rising briefly after the control signal is issued. Although minor, this transient overshoot reflects the dynamic limitation of valve switching and the compressibility of the fluid under rapid pressurization.

In the pressure-holding phase, the proposed system maintains a stable pressure in the range of 1.9÷2.1 MPa for the required duration of 180 seconds. Afterward, the proposed system gradually decreases to zero, marking the end of the test cycle. It is noteworthy that the depressurization characteristics vary slightly between tests, depending on the operator's timing and method of triggering the pressure release.

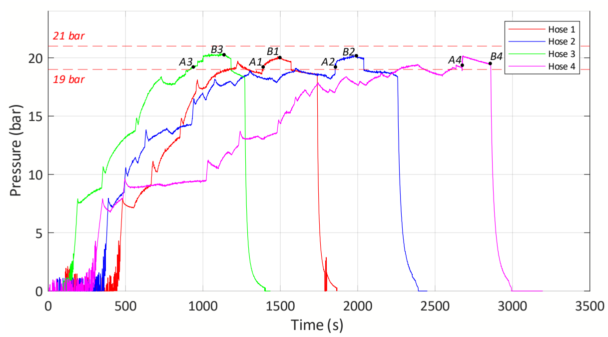

Figure 10 Hydrostatic pressure at the hose under high-leakage conditions

The trends in Figure 10 illustrate the variation of pressure in the D-HAST when connected to fire hose reels under high-leakage conditions. The data were collected over four separate test runs, and each curve clearly reflects three main phases: the pressurization phase from the start to point A, the hydrostatic pressure holding phase from point A to point B, where the target pressure is maintained for 180 seconds, and the depressurization phase from point B to the end of the cycle.

Compared to the results shown in Figure 9 under low-leakage conditions, both the duration of each phase and the total cycle time in Figure 10 are significantly extended. During the first 500 seconds, the hydrostatic pressure tends to fluctuate between 0 and approximately 0.43 MPa. This stage corresponds to the water-filling process, during which the hose is gradually inflated from a deflated initial state. Due to the flexible structure and uneven expansion characteristics of the hose, water fills each segment sequentially. As a section fills, the hydrostatic pressure rises momentarily, then drops again as the next segment begins to expand, resulting in continuous pressure oscillations during the early stage.

The actual pressurization phase begins only after the hose has been completely filled. This is the most time-consuming and unstable phase in the entire test process. The time required to reach the target pressure across the four test runs ranged from 964 to 2675 seconds. This wide variation is primarily attributed to differences in leakage rates at the hose couplings. Notably, in tests involving hose 1 and hose 4, although the hydrostatic pressure at the fire hose occasionally reached the desired level, it was unable to sustain it for the required duration. Due to excessive leakage, the hydrostatic pressure dropped again shortly after, forcing the pressure boosting system to restart the compensation process until the target pressure could be maintained continuously for 180 seconds.

The depressurization phase proceeded relatively smoothly and resembled that of the low-leakage case. However, an unusual phenomenon was observed during the first hose test. As the pressure approached zero, a slight reverse fluctuation occurred, with the hydrostatic pressure rising again to approximately 0.28 MPa. This behavior is explained by the sudden contraction of a section of the long hose during pressure release, which pushed water back into the system and caused a temporary pressure increase. This mechanism is similar to the oscillations observed in the early stages of the pressurization process.

4.0 CONCLUSION

This study proposed and validated a novel dual-hydraulic actuation system (D-HAST), specifically designed for testing hydrostatic pressure on sealed water containing samples with undefined expansion capabilities. By using the alternating operation of two hydraulic cylinders based on a control scheme driven by a Finite State Machine (FSM), this proposed principle effectively addresses the challenges associated with testing flexible, firefighting samples with varying internal volumes, such as fire hoses.

Experimental results demonstrate that, under low-leakage conditions, the D-HAST can rapidly pressurize the specimen, maintain stable target pressure over extended durations, and meet applicable inspection standards. Conversely, when testing hoses with significant leakage, the proposed system exhibits high sensitivity to pressure fluctuations, extended pressurization time, and inability to sustain target pressure, allowing a clear distinction between compliant and defective specimens.

Although the proposed D-HAST has demonstrated leakage compensated operation and compliance with hydrostatic pressure requirements specified in the standards, the current system still relies solely on pressure variation to infer leakage behavior. This approach does not provide real time information on instantaneous leakage flow, which limits the controller's ability to respond dynamically to pressure loss. Therefore, future development will focus on integrating a solution capable of evaluating leakage flow in real time and utilizing this parameter to establish a quantitative relationship between leakage rate, oil pump speed, and water pump compensation flow. These enhancements are expected to enable more precise regulation of output pressure and adaptive compensation under varying leakage conditions. In addition, the modular architecture of the D-HAST offers strong potential for industrial-scale implementation, where increased cylinder capacity, higher pump flow, and upgraded control power can extend its applicability to larger and more demanding hydrostatic testing scenarios.

Acknowledgement

This research is funded by Vietnam National University Ho Chi Minh City (VNU-HCM) under grant number TX2025b-20-01. We acknowledge the support of time and facilities from Key Laboratory of Digital Control and System Engineering (DCSELab), Ho Chi Minh City University of Technology (HCMUT), VNU-HCM for this study.

Conflicts of Interest

The author(s) declare(s) that there is no conflict of interest regarding the publication of this paper.

References

[1] C.-H. Bang, 2015. "A Study on Effects of Active Cooling Method on Human Body Wearing Firefighting Protection Equipment - Focusing on Using Ice-vest-," *Journal of the Korean Society of Hazard Mitigation* 15(1): 207–213. [Online]. DOI: 10.9798/KOSHAM.2015.15.1.207.

[2] A. Alayed, R. Alidrisi, E. Feras, S. Aboukozzana, and A. Alomayri, 2024. "Real-Time Inspection of Fire Safety Equipment using Computer Vision and Deep Learning," *Engineering, Technology & Applied Science Research*, 14(2): 13290–13298, Apr. DOI: https://doi.org/10.48084/etasr.6753.

[3] J. H. Heinbach and A. Aziz, 2024, "Automated Inspection of Obstructed Fire Extinguishers Using Amodal Instance Segmentation," Sep. *Technische Universität Hamburg, Institut für Digitales und Autonomes Bauen*. 325–332 DOI: 10.15480/882.13512.

[4] National Fire Protection Association (NFPA), 2023. "NFPA 25: Standard for the Inspection, Testing, and Maintenance of Water-Based Fire Protection Systems," National Fire Protection Association

[5] M. E. Kalaw, J. M. Kalaw, and M. A. Promentilla, 2021 "Geopolymers Synthesized from Philippine Coal Ash as Sustainable Alternative Low Heat Transmission and Fire-resistant Material for Buildings," *ASEAN Engineering Journal*, 11(3): 45–56. DOI: 10.11113/aej.v11.16871.

[6] P. Panedpojaman and T. Pothisiri, 2011, "Fire Resistance Evaluation for The Steel Roof Structure of A Typical Warehouse," *ASEAN Engineering Journal*, 1(3): 113–125. DOI: 10.11113/aej.v1.15302.

[7] X. Quang Ngo, T. Nguyen Chau, C. Thang Doan, V. T. Duong, D. V. Hoang, and T. Tien Nguyen, "Design of Mobile Manipulator for Fire Extinguisher Testing. Part I Key Specifications and Conceptual Design," *arXiv e-prints*, p. arXiv:2301.10965, Jan. 2023, DOI: 10.48550/arXiv.2301.10965.

[8] T. Nguyen Chau, X. Quang Ngo, V. T. Duong, T. T. Nguyen, H. H. Nguyen, and T. Tien Nguyen, 2023, "Design of Mobile Manipulator for Fire Extinguisher Testing. Part II: Design and Simulation," *arXiv e-prints*, p. arXiv:2301.10966. DOI: 10.48550/arXiv.2301.10966.

[9] International Organization for Standardization, 2009. "ISO-7165-Fire Fighting - Portable Fire Extinguishers - Performance and Construction," International Organization for Standardization.

[10] International Organization for Standardization, 2008. "ISO-11601-Fire Fighting - Wheeled Fire Extinguishers - Performance and Construction," International Organization for Standardization.

[11] H. D. Ho, H. N. Nguyen, C. T. Truong, V. T. Duong, and H. H. Nguyen, 2024, "Modeling and Control of Testing Machine for Fire Sprinkler K - Factor Evaluation," in *13th International Conference on Control, Automation and Information Sciences (ICCAIS)*. 1–6. DOI: 10.1109/ICCAIS63750.2024.10814215.

[12] International Organization for Standardization, 2014. "ISO 6182-1-Fire Protection - Automatic Sprinkler Systems, Part 1: Requirements and Test Methods for Sprinklers," International Organization for Standardization.

[13] H. D. Ho, H. N. Nguyen, C. T. Truong, V. T. Duong, T. T. Nguyen, and H. H. Nguyen, 2025. "Development of a System for Testing the Explosion Resistance of Portable Fire Extinguisher Cylinders under Hydrostatic Pressure," *International Review of Mechanical Engineering (IREME)*, 19(2): 94. DOI: 10.15866/ireme.v19i2.26026.

[14] H. H. Nguyen, C. T. Duong, H. L. Phan, T. T. Nguyen, V. T. Duong, and T. T. Nguyen, 2024, "Model Identification of Gas-Fired Industrial Furnace," in *AETA 2022—Recent Advances in Electrical Engineering and Related Sciences: Theory and Application*, T. Trong Dao, V. Hoang Duy, I. Zelinka, C. S. T. Dong, and P. T. Tran, Eds., Singapore: Springer Nature Singapore, 3–13.

[15] D. A. Simpson, 2020 "Comparative Risks of Hydrostatic and Pneumatic Pipeline Testing," *Journal of Pressure Vessel Technology.* 142(5): 054503. DOI: 10.1115/1.4046981.

[16] National Fire Protection Association (NFPA), 1962. "NFPA 1962 Standard for the Care, Use, and Service Testing of Fire Hose Including Couplings and Nozzles," [Online]. Available: www.nfpa.org,

[17] International Organization for Standardization, 2015. "ISO 4642-1-Rubber and plastics hoses, non-collapsible, for fire-fighting service, Part 1: Semi-rigid hoses for fixed systems," International Organization for Standardization. [Online]. Available: www.iso.org

[18] International Organization for Standardization, 2015. "ISO 4642-2-Rubber and Plastics Hoses, Non-collapsible, for Fire-Fighting Service, Part 2: Semi-rigid Hoses (and hose assemblies) for Pumps and Vehicles," [Online]. International Organization for Standardization. Available: www.iso.org

[19] Karolina Dwórska, Leszek Jurecki, Mateusz Jakubowski, 2023. Maksymilian Żurawski, and Łukasz Pastuszka, "Influence of External Factors on the Strength of Firefighting Hoses Used in Fire Protection Units," *Safety and Fire Technology*, 62(2): 150–170. DOI: 10.12845/sft.62.2.2023.9.

[20] M. N. Huynh, Q. M. Lam, C. T. Truong, H. H. Nguyen, and V. T. Duong, 2025. "Low-cost Electronic DC Load Module Design for Battery Capacity Evaluation," *HardwareX*, 23: e00679. DOI: 10.1016/j.ohx.2025.e00679.

[21] H. H. Nguyen, Q. M. Lam, T. T. Nguyen, V. T. Duong, and T. T. Nguyen. 2023. "Decision-Making Controller Based on a Finite State Machine for Emergency Call Redirection System in Elevator Intercoms," *International Review of Electrical Engineering (IREE)*, 18(2): 155. DOI: 10.15866/iree.v18i2.23480.

[22] J. Watton, 2009. *Fundamentals of Fluid Power Control*. Cambridge: Cambridge University Press, DOI: 10.1017/CBO9781139175241.

[23] J. S. Cundiff, 2001. *Fluid Power Circuits and Controls*. CRC Press. DOI: 10.1201/9781420041330.

[24] I. E. Idelchik, 2007. *Handbook of Hydraulic Resistance*, 4th ed. New York: Begell House.